Electronic Supplementary Information

Screening for cerebral amyloid angiopathy based on serological biomarkers analysis using a dielectrophoretic force-driven biosensor platform

Hye Jin Kim[a], Dongsung Park[a], Gyihyaon Yun[b], Hongrae Kim[a], Hyug-Gi Kim[c], Kyung Mi Lee[c], Il Ki Hong[d], Key-Chung Park[e], Jin San Lee[e], and Kyo Seon Hwang[a]

[a]Department of Clinical Pharmacology and Therapeutics, College of Medicine, Kyung Hee University, Seoul 02447, Republic of Korea

[b]Department of Medicine, Graduate School, Kyung Hee University, Seoul 02447, Republic of Korea

[c]Department of Radiology, Kyung Hee University Hospital, College of Medicine, Kyung Hee University, Seoul 02447, Republic of Korea

[d]Department of Nuclear Medicine, Kyung Hee University Hospital, College of Medicine, Kyung Hee University, Seoul 02447, Republic of Korea

[e]Department of Neurology, Kyung Hee University Hospital, College of Medicine, Kyung Hee University, Seoul 02447, Republic of Korea

Corresponding author

Kyo Seon Hwang, PhD

Department of Clinical Pharmacology and Therapeutics, Kyung Hee University College of Medicine, #26 Kyunghee-daero, Dongdaemun-gu, Seoul 02447, Republic of Korea

Tel: +82-2-961-9676, E-mail: k.hwang@khu.ac.kr

Co-Corresponding author

Jin San Lee, MD, PhD

Department of Neurology, Kyung Hee University Hospital, #23 Kyunghee-daero,

Dongdaemun-gu, Seoul 02447, Republic of Korea

Tel: +82-2-958-8499, E-mail: xpist@naver.com

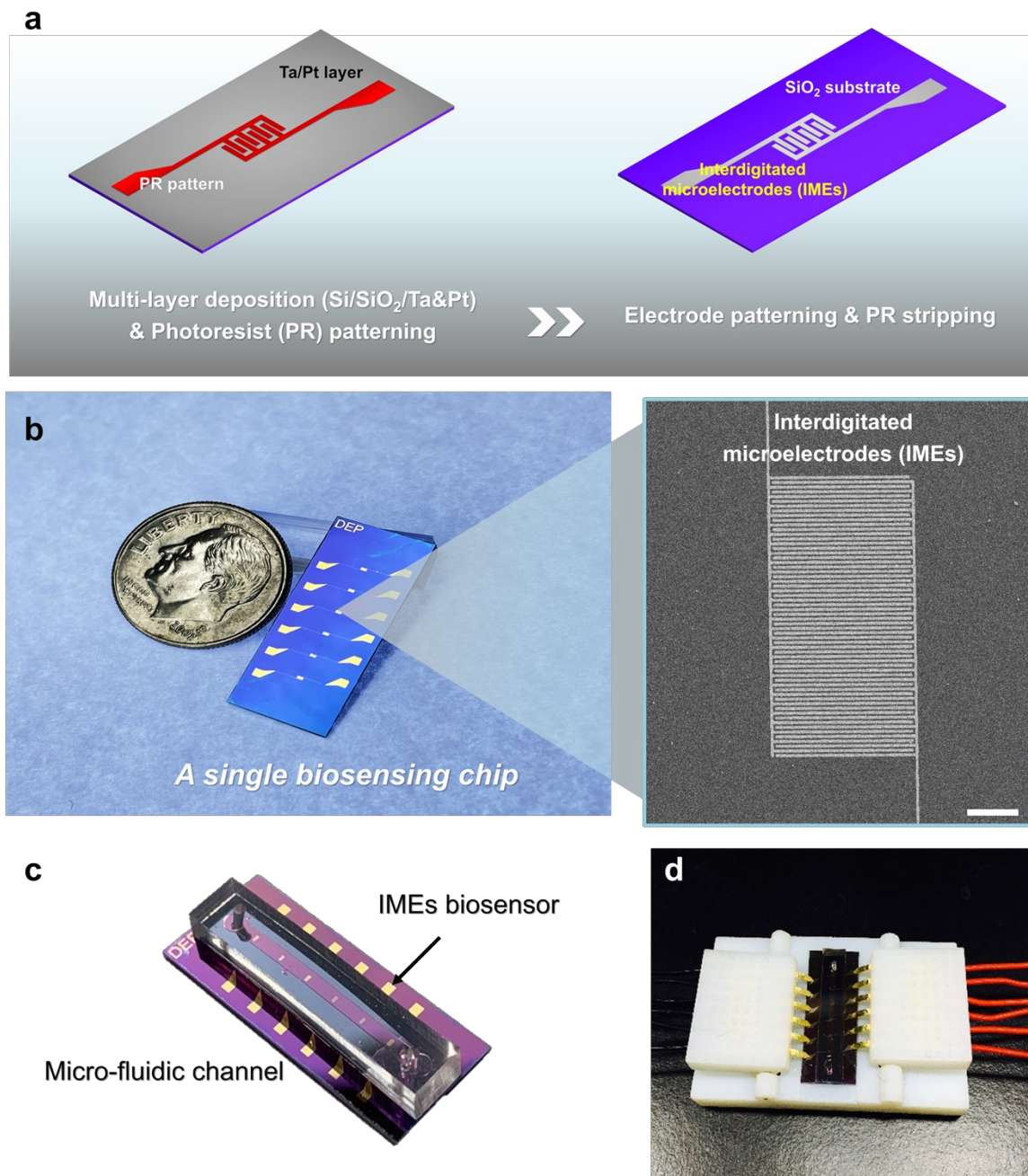**Fabrication process of DEP force-driven highly sensitive biosensor**

Figure S1. Fabrication of DEP force-driven biosensor. **(a)** Fabrication process of sensor via MEMS process, **(b)** images of the fabricated biosensor. Scale bar: 100 um, the single chip with **(c)** with attached microfluidics channel and **(d)** loaded on the measurement jig.
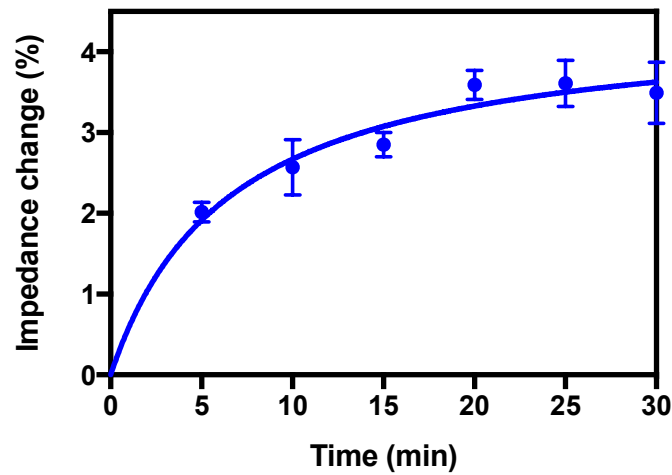
Optimization of antibody-target reaction time

Figure S2. Impedance change by specific binding of 10 pg/mL Aβ according to the applied time of DEP force.

When the DEP force was applied to the biosensor for 5 min, the impedance change was approximately $2.015 \pm 0.119\%$ and saturated to $3.591 \pm 0.182\%$ after 20 min. Accordingly, the reaction time was adjusted to 20 min, considering that the efficiency of concentration induced by DEP forces was saturated after 20 min.

Optimized time for sensor' signal stabilization

In order to optimize DEP application condition time, the effect of error and fluctuation of the biosensor's output signal was minimized by repeatedly checking the impedance signal stabilization time and setting the optimal impedance analysis condition.
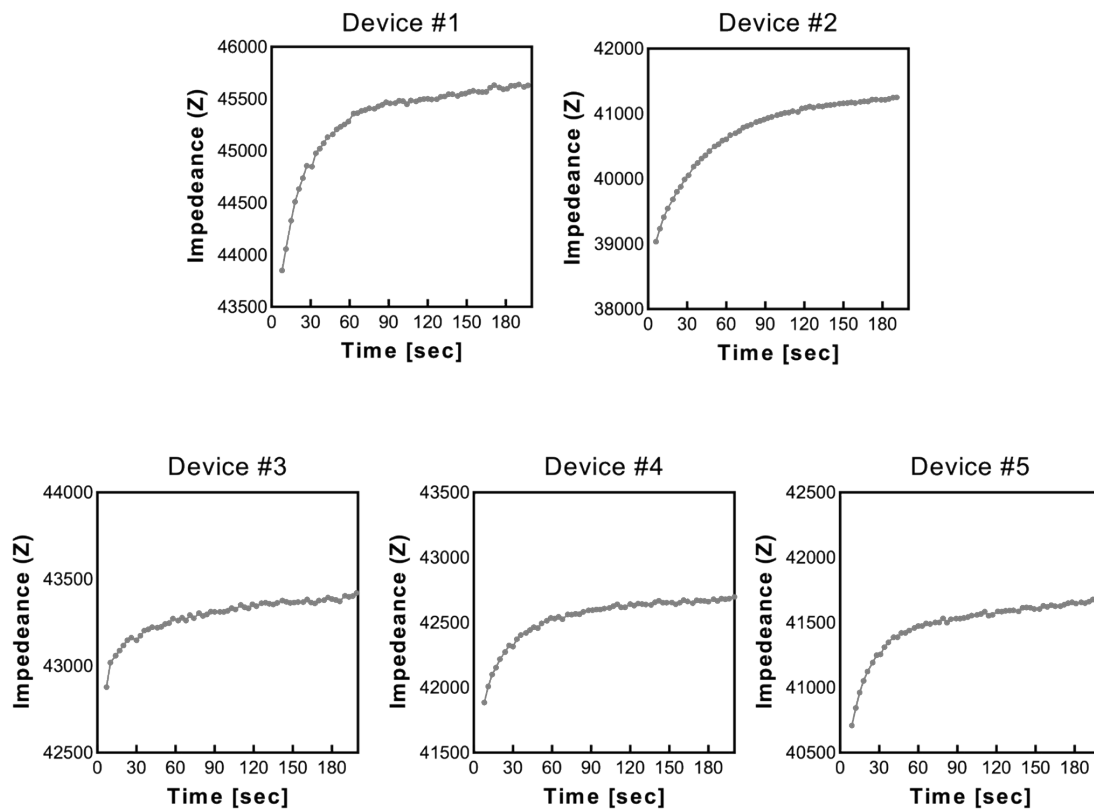

Figure S3. The impedance value of the 5 different biosensors.

From the five different biosensors, the signals from the sensors initially fluctuated but eventually saturated within 180 seconds. Consequently, based on 180 seconds, the fluctuation for 10 seconds back and forth was measured as $0.0252 \pm 0.008\%$.

Measurement frequency Optimization

The measurement frequency was optimized by analyzing the impedance change due to the specific binding of Aβ with concentration of 10 pg/mL in various frequency conditions.
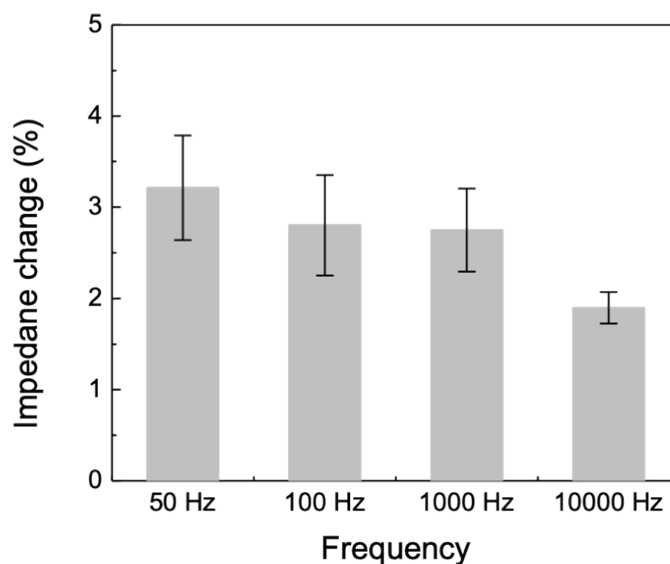

Figure S4. The impedance changes in various measurement frequency conditions.

As a result, it was confirmed that the sensitivity of the sensor increased as the frequency decreased. Such results are sufficiently reasonable considering that antibody immobilized at the surface of SiO_2 between the biosensor electrodes and a reaction of antibody-antigen occurred under 10 nm on the SiO_2. Therefore, the impedance of the sensor was measured in the low range, especially at 1,000 Hz, where the CV value is the lowest (50 Hz was not considered because there was noise generated from AC source (60 Hz in case of south Korea)).

Table S1. Average signal changes according to the concentration of Aβs

Concentrations (pg/mL)	In PBS (%)		In plasma (%)	
	$A\beta_{1-40}$	$A\beta_{1-42}$	$A\beta_{1-40}$	$A\beta_{1-42}$
0.01	3.609 (0.401)	1.563 (0.169)	4.126 (0.369)	3.627 (0.201)
0.1	5.402 (0.263)	1.950 (0.310)	5.119 (0.102)	4.293 (0.513)
1	6.739 (0.709)	2.235 (0.372)	5.969 (0.472)	4.548 (0.588)
10	7.583 (0.607)	3.176 (0.436)	6.784 (0.574)	5.649 (0.655)
100	8.599 (0.345)	3.392 (0.469)	8.476 (0.935)	6.836 (0.657)

Values are means (SD).
Abbreviation: Aβ, amyloid-β

Noise level of the biosensor by non-specific binding of plasma proteins and buffer exchange.
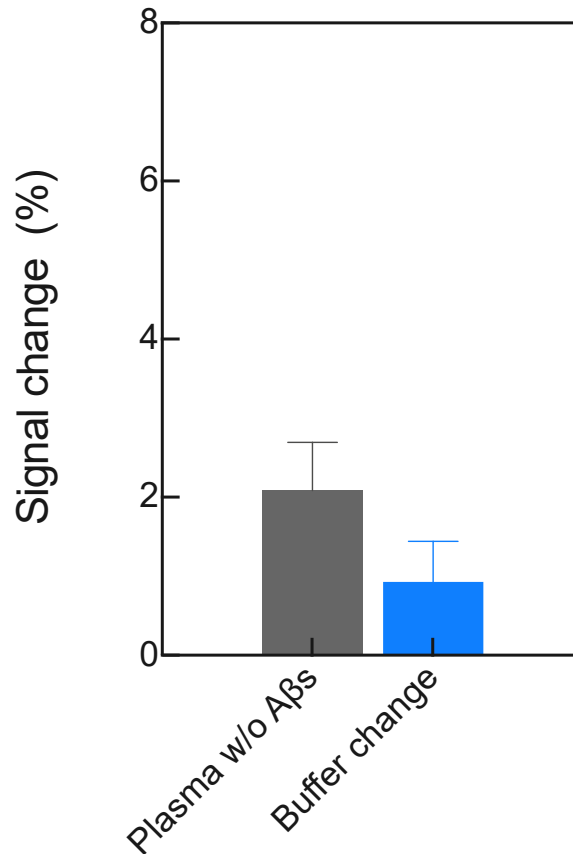

Figure S5. Noise level of the biosensor by non-specific binding of plasma proteins and buffer exchange. $A\beta$ = amyloid-β.

The result showed the impedance change of the biosensors by non-specific binding of numerous biomolecules presented in the standard plasma ("Plasma w/o $A\beta$", gray column) and by buffer exchange ("Buffer change" blue column), respectively. The signal of "Plasma w/o $A\beta$" was measured by injecting standard plasma without $A\beta$ spike into the microfluidic chip attached to the sensor surface and then reacting. Meanwhile, the signal of "Buffer change" was measured by injecting the pure PBS buffer without $A\beta$ spike into the microfluidic chip attached to the sensor surface and then reacting. Each signal change was approximately $2.086 \pm 0.585\%$

and 0.927 ± 0.490%, respectively, and among the signal changes, we defined the signal level

of "Plasma w/o Aβ" as noise level).

Differential diagnosis of the non-AD and AD groups using the level of (a) Aβ$_{1-40}$ and (b)

Aβ$_{1-42}$.

(a)

(b)

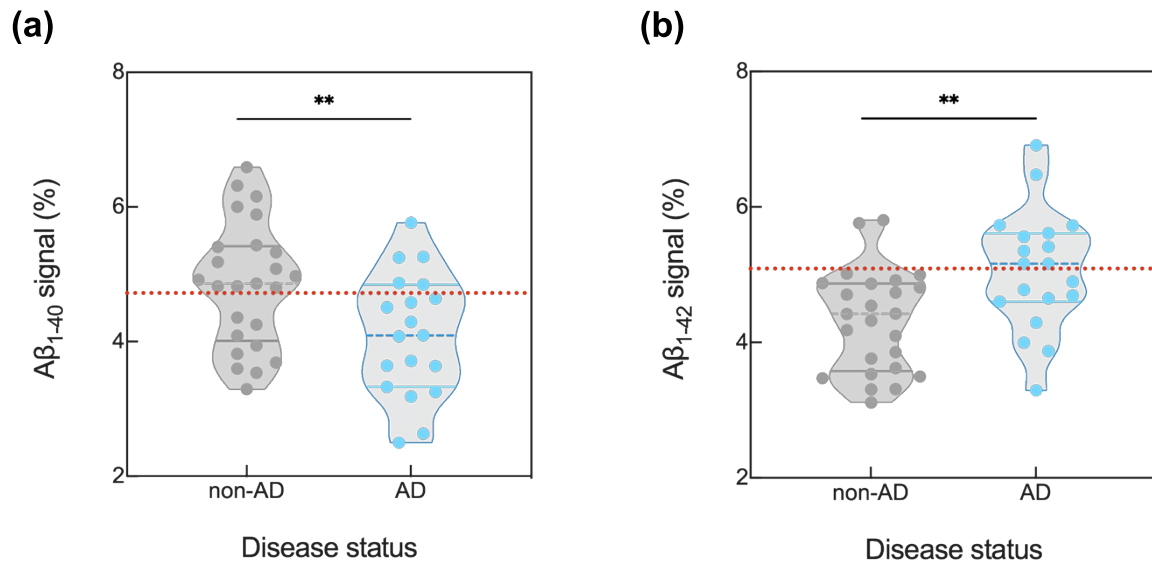**Figure S6. Differential diagnosis of the non-AD and AD groups using the level of (a) Aβ$_{1-40}$ and (b) Aβ$_{1-42}$.** non-AD = non-Alzheimer's disease; AD = Alzheimer's disease; Aβ = amyloid-β.

In the non-AD and AD groups the average signal levels of Aβ$_{1-40}$ (a) are approximately $4.846 \pm 0.453\%$ and $4.109 \pm 0.441\%$, respectively ($^{**}p < 0.01$, one-way ANOVA), while the levels of Aβ$_{1-42}$ (b) are approximately $4.320 \pm 0.366\%$ and $5.063 \pm 0.429\%$, respectively ($^{**}p < 0.01$, one-way ANOVA).

Receiver operating characteristic analysis in the non-AD and AD groups using the level of (a) $A\beta_{1-42}/A\beta_{1-40}$, (b)$A\beta_{1-40}$ and (c) $A\beta_{1-42}$.

(a)

(b)   **(c)**

Figure S7. Receiver operating characteristic analysis in the non-AD and AD groups using the level of (a) $A\beta_{1-42}/A\beta_{1-40}$, (b)$A\beta_{1-40}$ and (c) $A\beta_{1-42}$. non-AD = non-Alzheimer's disease; AD = Alzheimer's disease; $A\beta$ = amyloid-β.
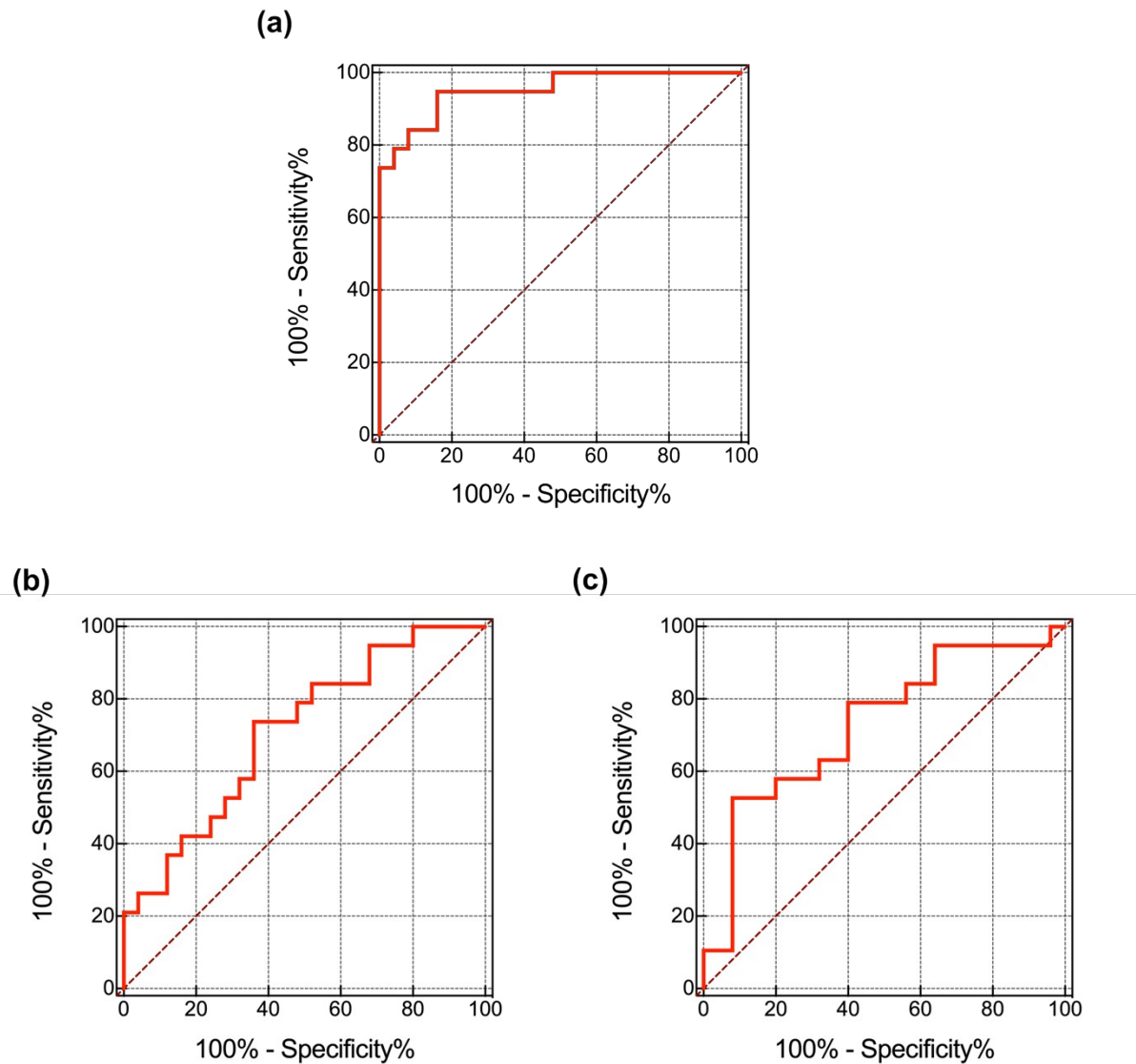
The area under the curve values are approximately (a) 0.95 (95% CI 0.89–1.00) (b) 0.71 (95% CI 0.56–0.86) and (c) 0.73 (95% CI 0.57–0.88).

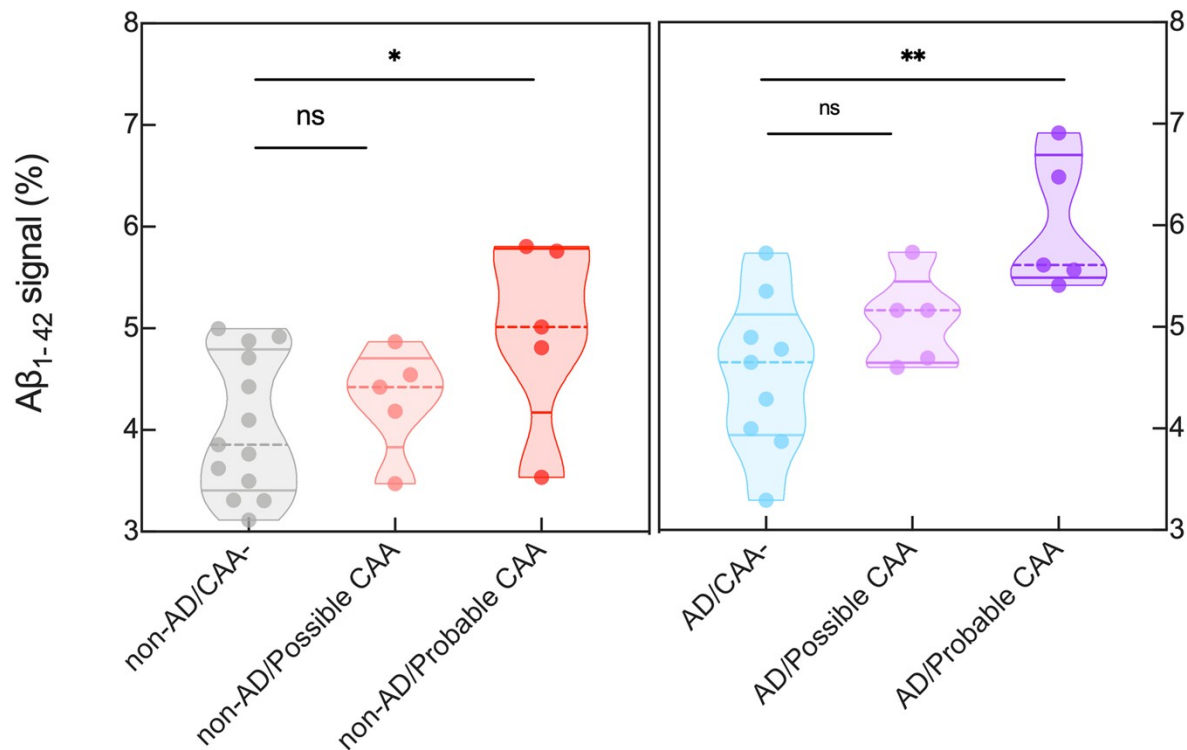**Levels of Aβ$_{1-42}$ in the non-AD and AD groups according to the severity of CAA**

Figure S8. Levels of Aβ$_{1-42}$ in the non-AD and AD groups according to the severity of CAA, non-AD = non-Alzheimer's disease; CAA = cerebral amyloid angiopathy; AD = Alzheimer's disease; Aβ = amyloid-β.

Although the signal level of Aβ$_{1-42}$ increased with the severity of CAA, the significant difference among the groups is lower than that of Aβ$_{1-40}$. The average signal level of Aβ$_{1-42}$ in the NC/probable CAA group was higher than the non-AD/CAA- group ($^{*}p < 0.05$, one-way ANOVA), whereas there was no significant difference between the non-AD/CAA- and NC/possible CAA groups (ns=non-significant, one-way ANOVA). Similarly, Aβ$_{1-42}$ levels between the AD/CAA- and AD/probable CAA groups appear to be significant ($^{**}p<0.01$, one-way ANOVA), but there is no difference in levels between the AD/CAA- and AD/possible CAA groups (ns=non-significant, one-way ANOVA).

Table S2. Demographics and plasma Aβ analysis of the study participants

	Total	Non-AD					AD				
		Total non-AD	CAA-	CAA+			Total AD	CAA-	CAA+		
				Total	Possible CAA	Probable CAA			Total	Possible CAA	Probable CAA
N	44 (100)	25 (56.8)	15 (60.0)	10 (40.0)	5 (50.0)	5 (50.0)	19 (43.2)	9 (47.4)	10 (52.6)	5 (50.0)	5 (50.0)
Age, years	69.7 (8.0)	68.4 (6.5)	64.9 (5.0)[b]	73.6 (4.8)	75.2 (3.7)	72.0 (5.6)	71.5 (9.5)	69.7 (9.6)	73.1 (9.6)	66.4 (8.8)	79.8 (4.2)
Female	31 (70.5)	17 (68.0)	9 (60.0)	8 (80.0)	4 (80.0)	4 (80.0)	14 (73.7)	6 (66.7)	8 (80.0)	5 (100.0)	3 (60.0)
Education, years	9.4 (5.6)	10.2 (6.2)	10.8 (6.9)	9.2 (5.4)	8.1 (4.7)	10.2 (6.3)	8.5 (4.7)	8.6 (5.4)	8.4 (4.2)	7.8 (5.0)	9.0 (3.7)
APOE ε4 status	18 (40.9)	8 (32.0)	5 (33.3)	3 (30.0)	1 (20.0)	2 (40.0)	10 (52.6)	6 (66.7)	4 (40.0)	3 (60.0)	1 (20.0)
Hypertension	27 (61.4)	18 (72.0)	10 (66.7)	8 (80.0)	5 (100.0)	3 (60.0)	9 (47.4)	4 (44.4)	5 (50.0)	2 (40.0)	3 (60.0)
DM	15 (34.1)	8 (32.0)	3 (20.0)	5 (50.0)	4 (80.0)	1 (20.0)	7 (36.8)	4 (44.4)	3 (30.0)	1 (20.0)	2 (40.0)
Dyslipidemia	25 (56.8)	14 (56.0)	8 (53.3)	6 (60.0)	4 (80.0)	2 (40.0)	11 (57.9)	4 (44.4)	7 (70.0)	3 (60.0)	4 (80.0)
MMSE	21.8 (56.0)	25.1 (4.6)[a]	27.2 (2.2)[b]	21.9 (5.5)	21.4 (3.6)	22.4 (7.4)	17.5 (4.8)	17.1 (4.9)	17.9 (5.0)	19.4 (3.5)	16.4 (6.2)
Aβ-PET SUVR	1.393 (0.259)	1.198 (0.059)[a]	1.174 (0.046)[b]	1.234 (0.060)	1.223 (0.065)	1.245 (0.061)	1.649 (0.182)	1.546 (0.116)[c]	1.742 (0.184)	1.653 (0.145)	1.831 (0.188)
Plasma Aβ, %											
Aβ$_{1-40}$	4.520 (0.967)	4.846 (0.906)[a]	4.466 (0.956)[b]	5.417 (0.505)	5.162 (0.242)	5.672 (0.594)	4.109 (0.881)	3.437 (0.605)[c]	4.714 (0.675)	4.363 (0.710)	5.066 (0.460)
Aβ$_{1-42}$	4.641 (0.871)	4.320 (0.733)[a]	4.105 (0.655)	4.643 (0.795)	4.299 (0.523)	4.986 (0.924)	5.063 (0.858)	4.540 (0.760)[c]	5.533 (0.722)	5.071 (0.453)	5.995 (0.660)
Aβ$_{1-42/1-40}$	1.059 (0.256)	0.904 (0.127)[a]	0.936 (0.139)	0.855 (0.101)	0.835 (0.114)	0.874 (0.095)	1.263 (0.238)	1.354 (0.318)	1.182 (0.118)	1.178 (0.140)	1.186 (0.106)

Values are means (SD) or N (%).
The value of plasma Aβ is the average impedance change of the biosensing platform.

Statistical analyses were performed using chi-square tests, Fisher's exact test, or Student's *t-test*.
[a]Difference between non-AD and AD, $p < 0.05$
[b]Difference between non-AD/CAA- and non-AD/CAA+ (total), $p < 0.05$.
[c]Difference between AD/CAA- and AD/CAA+ (total), $p < 0.05$.
Abbreviations: N, number; non-AD, non-Alzheimer's disease; AD, Alzheimer's disease; CAA, cerebral amyloid angiopathy; *APOE*, apolipoprotein E; DM, diabetes mellitus; MMSE, Mini-Mental State Examination; Aβ, amyloid-β; PET, positron emission tomography; SUVR, standardized uptake value ratio.

Supplementary Information Note 1: Sensing mechanism

Our sensors concentrate biomolecules through the interaction of the dielectrophoretic force (F_{DEP}) and drag force (F_{drag}), enabling highly sensitive biomolecules detection. When an alternating voltage (AC) of each frequency ($\omega = 2\pi f$) is applied, the biomolecules with radius R undergo the F_{DEP} with an intensity as follows:

$$F_{DEP} = 2\pi\varepsilon_m R^3 Re[f_{CM}(\omega)] \cdot |\nabla E_{rms}|^2 \tag{1}$$

where ε_m, $Re[f_{CM}(\omega)]$, and E refer to the medium permittivity (approximately $80 \cdot \varepsilon_0$), the real part of the Clausius–Mossotti (CM) factor, and the root-mean-squared field gradient ($|\nabla E_{rms}|^2$), respectively. Based on the information in Table The intensity of $|\nabla E_{rms}|^2$ between the IMEs was calculated using COMSOL Multiphysics ver. 5.2 (COMSOL Inc.), and the information used in the simulation are listed in Table S3.

Table S3. Material properties and layer thickness for numerical simulations

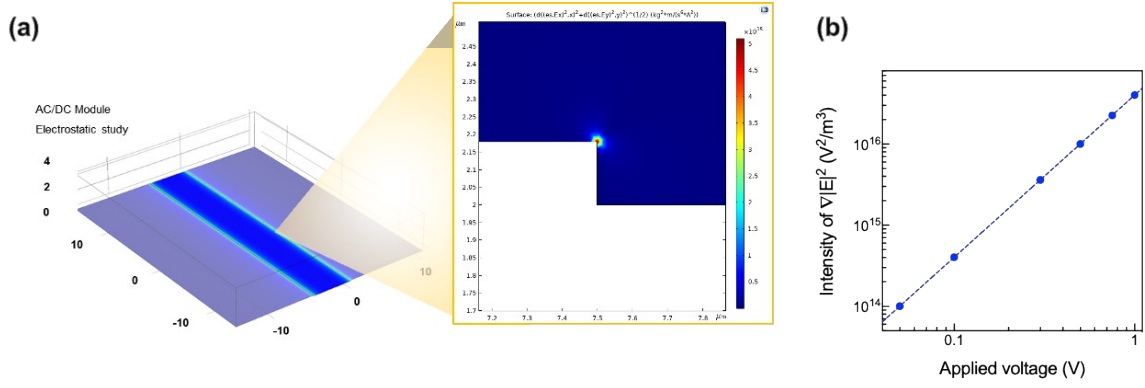| Materials	Dimension (m)	Permittivity (ε)	Conductivity (σ) [S·m^{-1}]
Water	-	$80 \cdot \varepsilon_0$	10^{-4}
Pt	*Gap* = 5 μm, *Thickness* = 180 nm	-	9.43×10^6
SiO$_2$	-	$3.9 \cdot \varepsilon_0$	10^6

Figure S9. (a) Distribution of a non-uniform electric field (E) on the surface of interdigitated microelectrode IMEs and **(b)** the intensity of the root-mean-squared field gradient (∇E^2) based on the applied voltage.

Also, the real part of the CM factor, which the control the direction of F_{DEP} was calculated using the following equation (2) – (4)[1]:

$$K(\omega) = \frac{\varepsilon_p^*(\omega) - \varepsilon_m^*(\omega)}{\varepsilon_p^*(\omega) + 2\varepsilon_m^*(\omega)} \tag{2}$$

$$\varepsilon_p^*(\omega) = \varepsilon_p^* - j\frac{\sigma_p}{\omega} \tag{3}$$

$$\varepsilon_m^*(\omega) = \varepsilon_m^* - j\frac{\sigma_m}{\omega} \tag{4}$$

where p and m denote the particle and medium, respectively, and ε and $\varepsilon^*(\omega)$ represent the pemittivities, complex permittivities, and conductivity, respectively. The relative permittivity and conductivity of Aβ were calculated using the following equation (5) and (6)[2], respectively, and the calculated and detail values were described in Table S4.

$$\varepsilon_r \left[F \cdot m^{-1}\right] = \frac{\sum_{i=1}^{n} \varepsilon_{unit}}{n} \tag{5}$$

$$\sigma_p \, [S \cdot m^{-1}] = K \cdot \frac{l}{A}$$

(6)

where, ε_{unit} and n donate the permittivity of unit amino acid residues[3] and the number of amino acid composed the protein, respectively, and K, l, and A represent the conductance of the protein (assumed to be 0.2 nS)[2] as well as height and cross-sectional area of the protein, respectively.

Table S4. Parameters for calculating the Clausius–Mossotti (CM) factor

Parameters	Values
Relative permittivity of Aβ, $\varepsilon_{r\_A\beta}$	16.8860 (Calculated)
Conductivity of Aβ, $\sigma_{A\beta}$	0.1169 (Calculated)
Relative permittivity of medium, Water, ε_{r_m}	80.1
Conductivity of medium (σ_m)	1×10^{-4} S·m^{-1}

Meanwhile, the intensity of F_{drag} acting opposite to the relative movement of the particle with respect to the surrounding fluid is obtained from the following equation:

$$F_{drag} = -6\pi\eta R u$$

(7)

where η and u represent the dynamic viscosity of the medium (8.9×10^{-4} Pa·s) and velocity of the particle, respectively. Using equations (1) and (7), the difference between $\mathbf{F}_{DEP}$ and $\mathbf{F}_{drag}$ can be calculated according to the intensity of $|\nabla E_{rms}|^2$.

1. Kim, D., Sonker, M., & Ros, A. (2018). Dielectrophoresis: From molecular to micrometer-scale analytes. Analytical chemistry, 91(1), 277-295.
2. Zhang, B., Song, W., Pang, P., Lai, H., Chen, Q., Zhang, P., & Lindsay, S. (2019). Role of contacts in long-range protein conductance. Proceedings of the National Academy of Sciences, 116(13), 5886-5891.

3. Li, L., Li, C., Zhang, Z., & Alexov, E. (2013). On the dielectric "constant" of proteins: smooth dielectric function for macromolecular modeling and its implementation in DelPhi. Journal of chemical theory and computation, 9(4), 2126-2136.